Supplementary Material (ESI) for ChemComm

A Novel Mesoporous Carbon@Silicon-Silica Nanostructure for High-Performance Li-ion Battery Anode

Qianjun He,*[a,b] Chaohe Xu,[a] Jianqiang Luo,[a] Wei Wu,[a] Jianlin Shi*[a]

[a] *State Key Laboratory of High Performance Ceramics and Superfine Microstructure, Shanghai Institute of Ceramics, Chinese Academy of Sciences, 1295 Ding-Xi Road, Shanghai 200050, China*

[b] *School of Chemistry, University of Leeds, Woodhouse Lane, Leeds LS2 9JT, UK*

* Correspondence should be addressed to Q.J. He. E-mail address: nanoflower@126.com

Experimental Section

Synthesis of MCSSNs

Firstly, 6.8 g of Pluronic P123 ($PEO_{20}PPO_{70}PEO_{20}$, BASF Co., Ltd.) and 12 g of NaCl (Sinopharm Chemical Reagent Co. Ltd., Shanghai) were fully dissolved into 200 mL of HCl solution (0.1 M) at 35 °C under intensive stirring and under argon blowing protection. Then 18 mL of triethoxysilane (TES, Alfa Aesar) was added dropwise. After 6 hours, the reaction solution in a white colloidal state was centrifugated for 10 min with the centrifugal force of 18000*g* in a high speed refrigerated centrifuge, and washed for three times with deionized water to remove residual reactants. The collected as-synthesized oxygen-deficient mesoporous silica nanoparticles (MSNs) were dispersed in deionized water and then the freeze drying power was collected in order to reduce the aggregation of nanoparticles. Finally, the freeze drying power was calcined for 3 hours at 900 °C at a heating rate of 2 °C min^{-1} under nitrogen protection to obtain the black product MCSSNs. In addition, in order to facilely determine the type of carbon, silicon and silica within MCSSNs were etching with HNO_3 (65%) and HF (40%) solutions in turn under stirring.

Characterization of MCSSNs

The morphology and mesostructure of nanoparticles were observed *via* transmission electron microscopy (TEM) and scanning electron microscopy (SEM), which were performed on a JEM–2010 electron microscope and a JSM-6700F electron microscope, respectively. Small-angle and wide-angle X-ray diffraction (SAXRD) data were recorded on a Rigaku D/Max-2550V diffractometer using Cu Kα radiation (40 kV and 40 mA) at a scanning rate of 0.4° min^{-1} over the range of 0.6–80°.

The porosity was measured by nitrogen adsorption–desorption isotherm experiments, which were carried out on a Micromeritics Tristar 3000 analyzer at 77 K under a continuous adsorption condition, with all samples dried for 12 h at 120 °C under nitrogen before measurements. Average pore diameter was calculated from desorption branches of the nitrogen adsorption–desorption isotherms by the Barrett–Joyner–Halenda (BJH) method, and specific surface area and pore volume were calculated by Brunauer–Emmett–Teller (BET) and BJH methods, respectively.

The thermal decomposition process of sample MSNs was measured by a TG thermal analyzer over the range of 30–1000 ºC at a heating rate of 5 °C min^{-1} in nitrogen.

The carbon content of MCSSNs was measured by CHN elemental analyses (Vario MICRO, Elementar Analysensysteme GmbH, Germany). FTIR spectra were collected on a Nicolet (Madison, WI) Magna 550 infrared spectrophotometer using KBr technique. Three hundred scans were collected per sample over the range of 3200 to 400 cm^{-1} at a resolution of 4 cm^{-1}. Raman spectra were recorded on a LabRAM HR800 laser Raman spectroscope (Jobin Yvon, France) under a radiation excitation wavelength of 632.8 nm at room temperature.

Electrochemical Measurements

The electrochemical properties of MCSSNs as the anode electrode used in Li-ion batteries were characterized at room temperature. The working electrode was composed of the active material MCSSNs, the conductive material acetylene black (AB) and the binder polyvinylidene fluoride (PVDF) in a weight ratio of MCSSNs:AB:PVDF = 80:10:10. Li foil was used as the counter electrode. The electrolyte solution was 1 M $LiPF_6$ in a 50:50 w/w mixture of ethylene carbonate (EC) and dimethyl carbonate (DMC). The cell assembly was carried out in a glovebox filled with pure argon (99.999%), in which the concentrations of moisture and oxygen were less than 1 ppm. The electrode activities were measured using a Land CT2001 battery tester. The cell was charged and discharged at different current densities in the potential of 1.5 V at room temperature. After 100 charge−discharge cycles, MCSSNs were detached from nanocomposite electrodes, ultrasonically dispersed into dimethylformamide (DMF) and washed several times with DMF, and observed by HR-TEM for their microstructures.

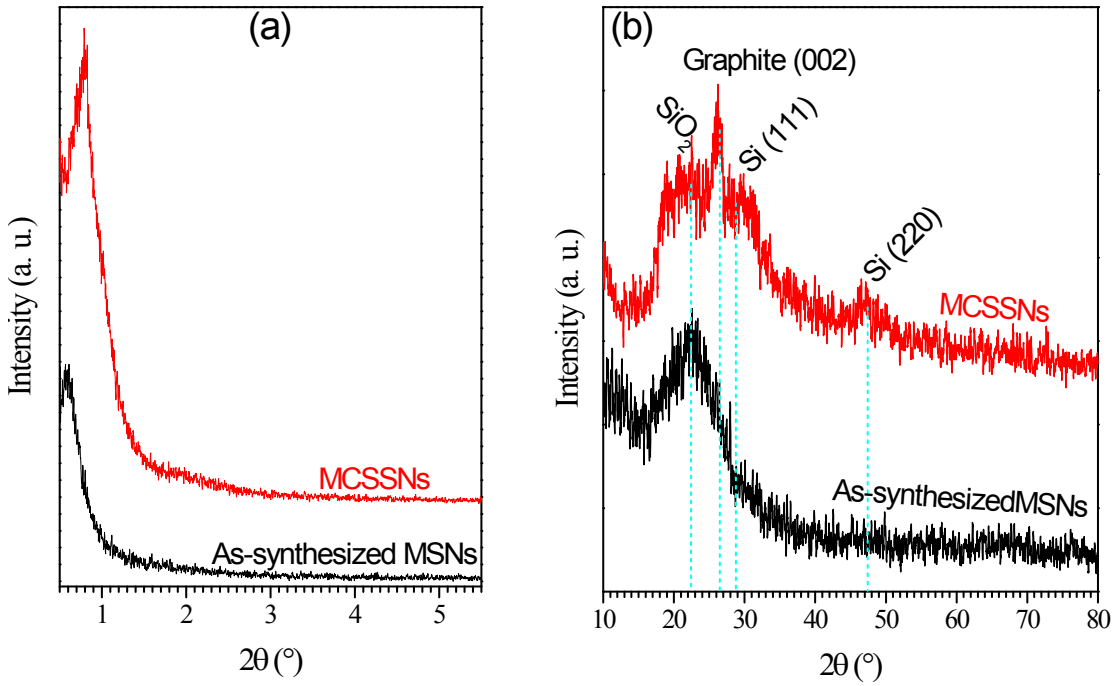

Supplementary Figure S1. Small-angle (a) and wide-angle (b) XRD patterns of the as-synthesized sample MSNs and the post-calcined sample MCSSNs. It could be found from the small-angle XRD peak shift towards high angle (a) that the mesopore interspace became smaller after calcination, which could result from the shrinkage of mesoporous walls during dehydrogenation.

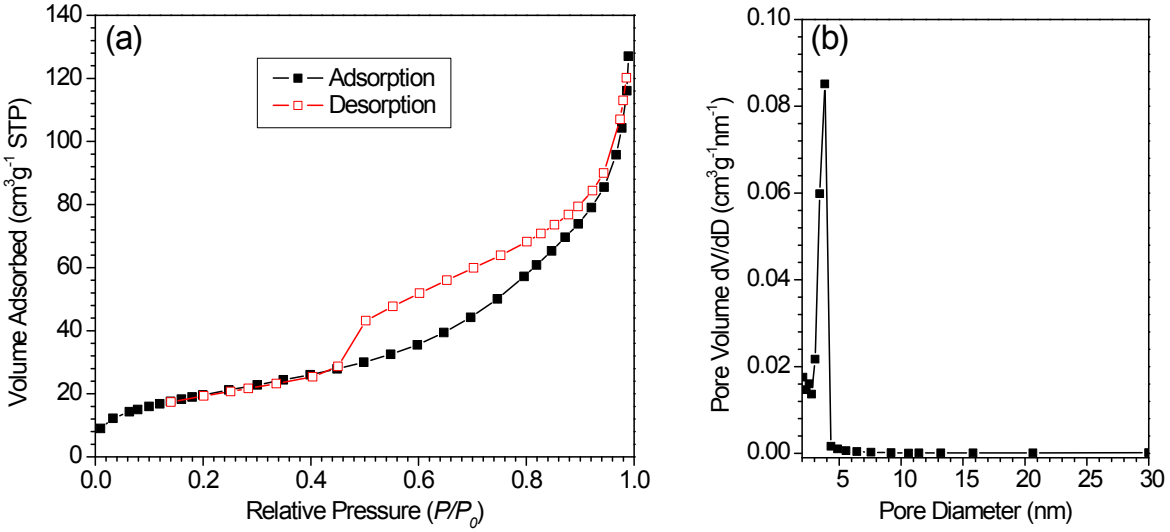

Supplementary Figure S2. Nitrogen adsorption–desorption isotherms (a) and pore size distribution curve (b) of MCSSNs. MCSSNs exhibit the classical type-IV adsorption–desorption isotherms with a type-H3 hysteresis loop, which indicates that MCSSNs possess a kind of slit-like mesoporous structure. Such slit-like mesoporous channels are believed to be constructed by the mesopores of silica and the inserted carbon, as shown by the hierarchical structure of MCSSNs in Scheme 1. In addition, the well-defined step loop at the relative pressures of 0.4–0.6 (figure a) and the narrow pore size distribution (figure b) suggest that MCSSNs possess a uniform mesoporous structure in accordance with the results obtained from TEM images and SA-XRD data.

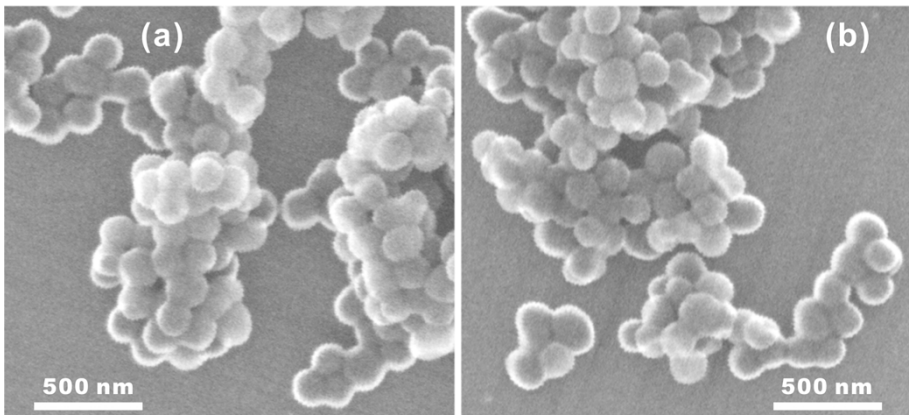

Supplementary Figure S3. SEM images of the as-synthesized sample MSNs (a) and the post-calcined sample MCSSNs (b).

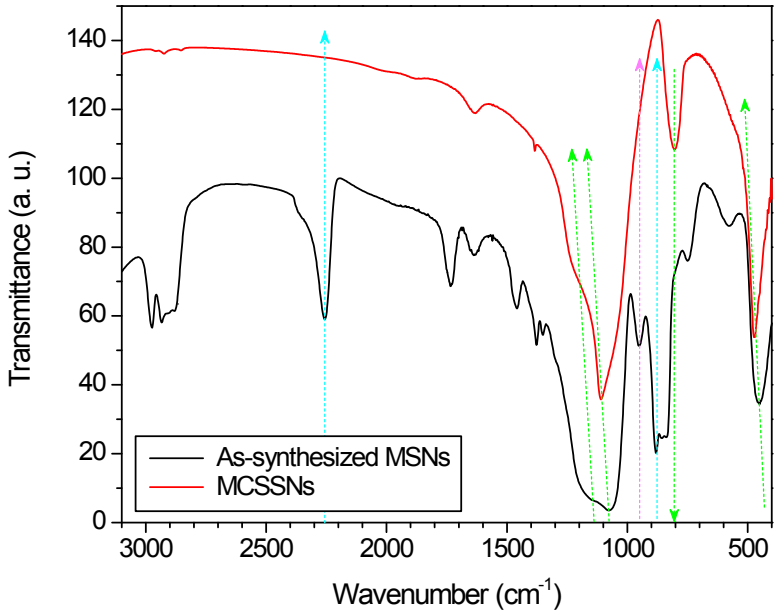

Supplementary Figure S4. FTIR spectra of the as-synthesized sample MSNs and the post-calcined sample MCSSNs. The as-synthesized sample MSNs shows two characteristic absorption bands of $O_3Si{-}H$ at 2255 cm^{-1} and 883 cm^{-1}, which are readily assigned to Si−H stretching and bending vibrations, respectively.[1] After calcination/crystallization at 900 °C, both peaks disappear (as indicated by the blue arrow), indicating the Si−H rupture. In addition, the 883 cm^{-1} band disappearance is also associated with the formation of Si–Si bond.[2] The as-synthesized sample MSNs also shows a weak absorption band at 950 cm^{-1}, which should be attributed to the Si−OH stretching of free silanols. After calcination at 900 °C, this Si−OH band disappeared (as indicated by the red arrow in Figure S6), indicating that the Si–O–Si network was contracted by the dehydration between Si−OH groups. Meanwhile, the rocking, internal TO (transverse optic) stretching and external LO (longitudinal optic) stretching vibrations of Si–O–Si were shifted towards long wavelength from 453 cm^{-1} to 474 cm^{-1}, from 1074 cm^{-1} to 1110 cm^{-1}, from 1145 cm^{-1} to 1200 cm^{-1}, respectively, and the rocking, bending (802 cm^{-1}) and internal TO stretching vibrations of Si–O–Si were intensified as compared with the external LO stretching vibration after calcination at 900 °C (as indicated by the green arrow). This suggests that the ordering degree of the $[SiO_4]$ tetrahedral network became high, which should owe to the crystallization of Si within the oxygen-deficient network of MSNs.

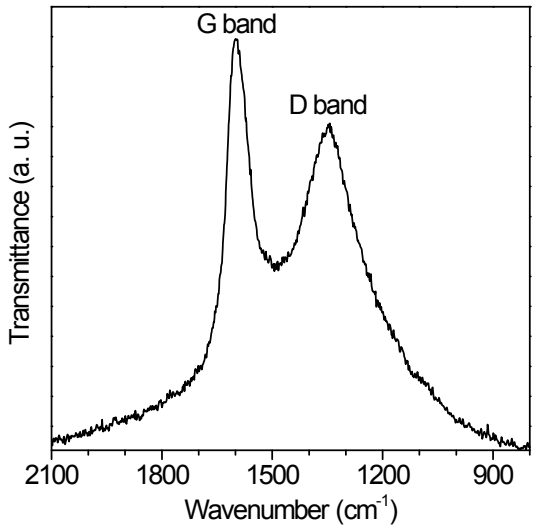

Supplementary Figure S5. Raman spectrum of carbon within MCSSNs.

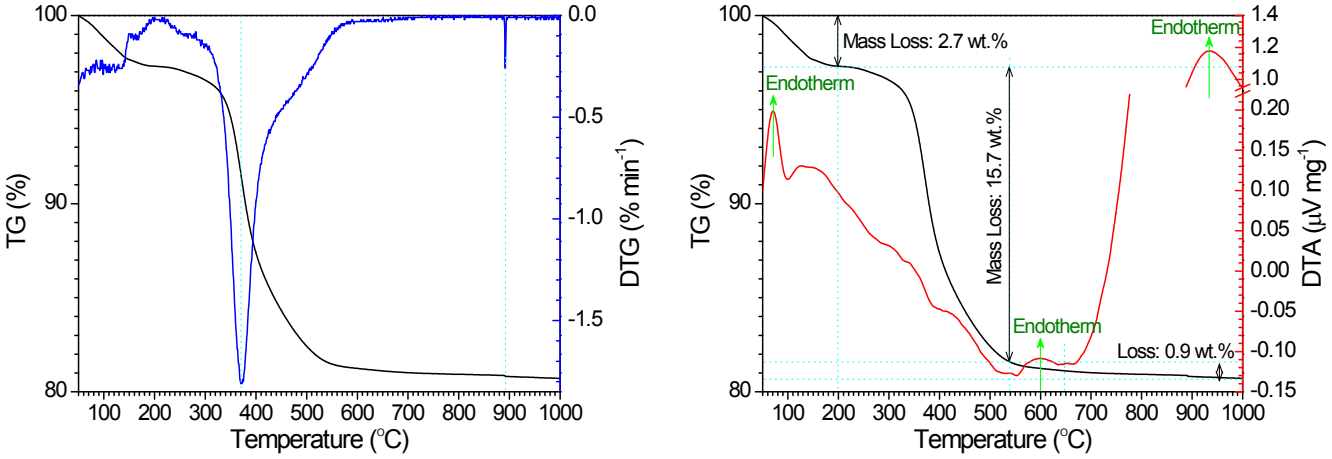

Supplementary Figure S6. TG/DTA/DTG curves of the as-synthesized MSNs. From TG/DTG curves, there are two sharp mass loss peaks centred at 370 °C and 890 °C, owing to the decomposition of P123 and the dehydrogenization of MSNs. Therefore, the calcination temperature was chose as 900 °C in this work to accomplish the decomposition/ dehydrogenization/ condensation of the as-synthesized MSNs. From TG/DTA curves, it can be found that the endothermic peak below 200 °C results from the dehydration, responding to 2.7 wt.% of mass loss; a series of exothermic peaks at 200~540 °C reflect the decomposition and dehydrogenization of the as-synthesized MSNs with 15.7 wt.% of mass loss; two endothermic peaks at 600 °C and 936 °C indicate the Si crystallization and the P123 carbonization.

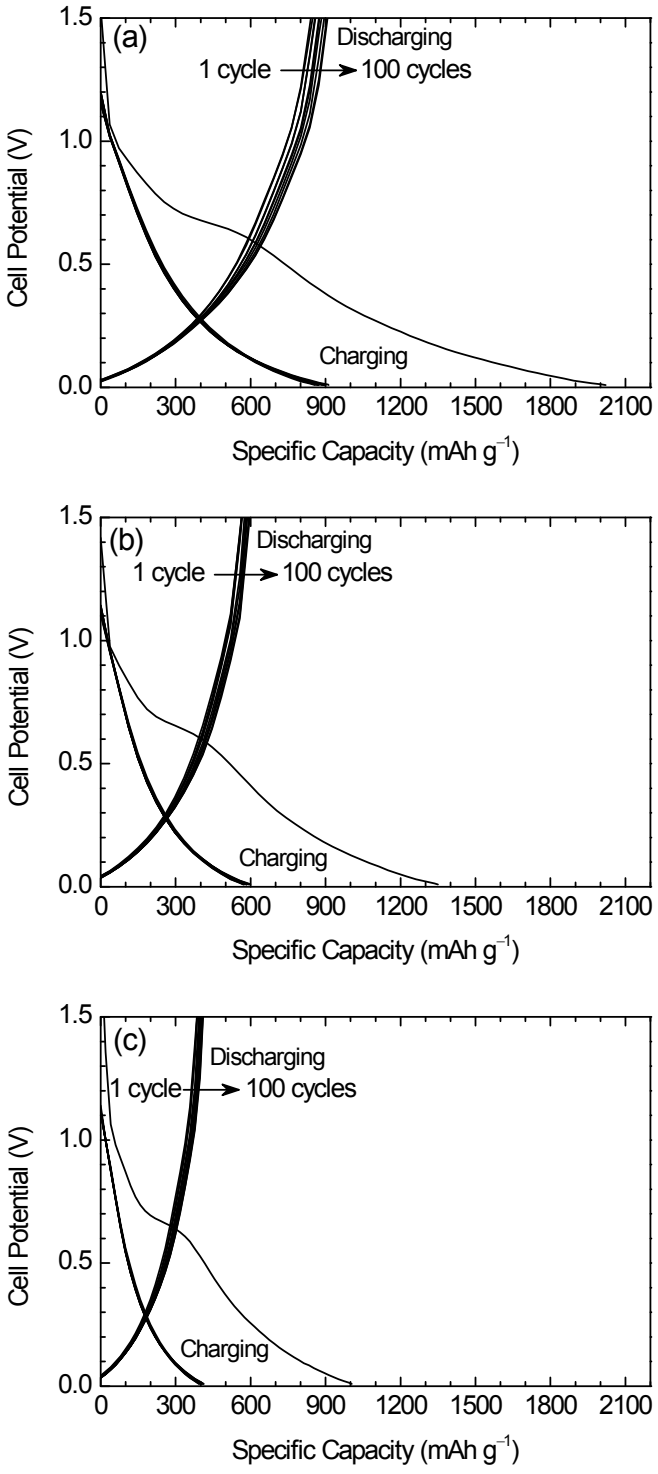

Supplementary Figure S7. Galvanostatic discharge−charge curves of MCSSNs electrodes cycled for 100 times at current densities of (a) 100 mA g^{-1}, (b) 150 mA g^{-1}, and (c) 500 mA g^{-1}.

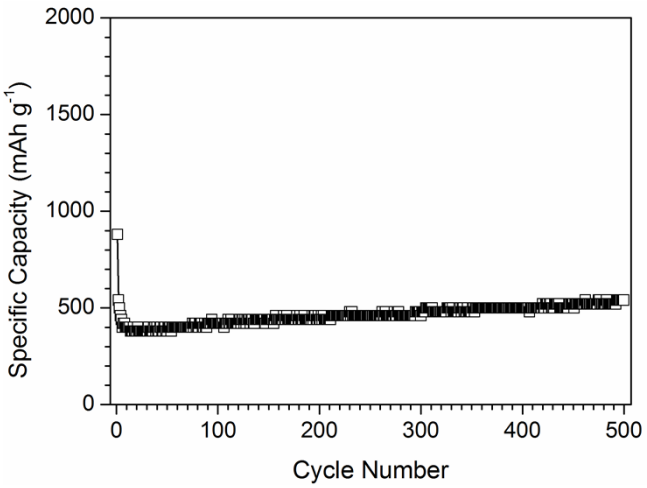

Supplementary Figure S8. Cyclability of MCSSNs electrodes at the current density of 500 mA g^{-1}.

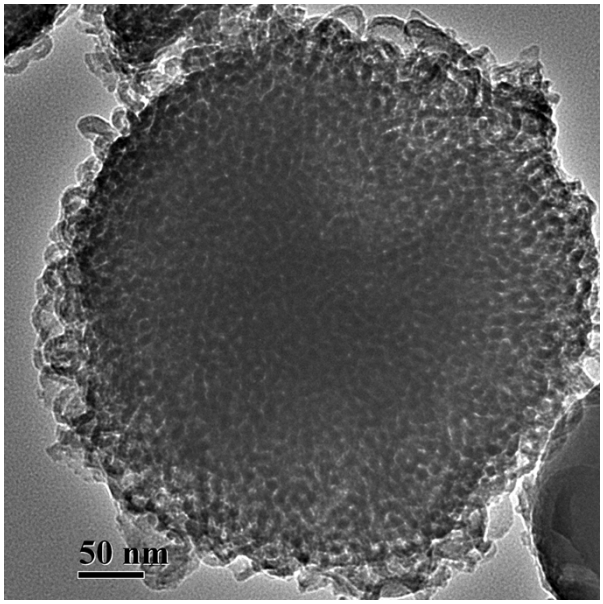

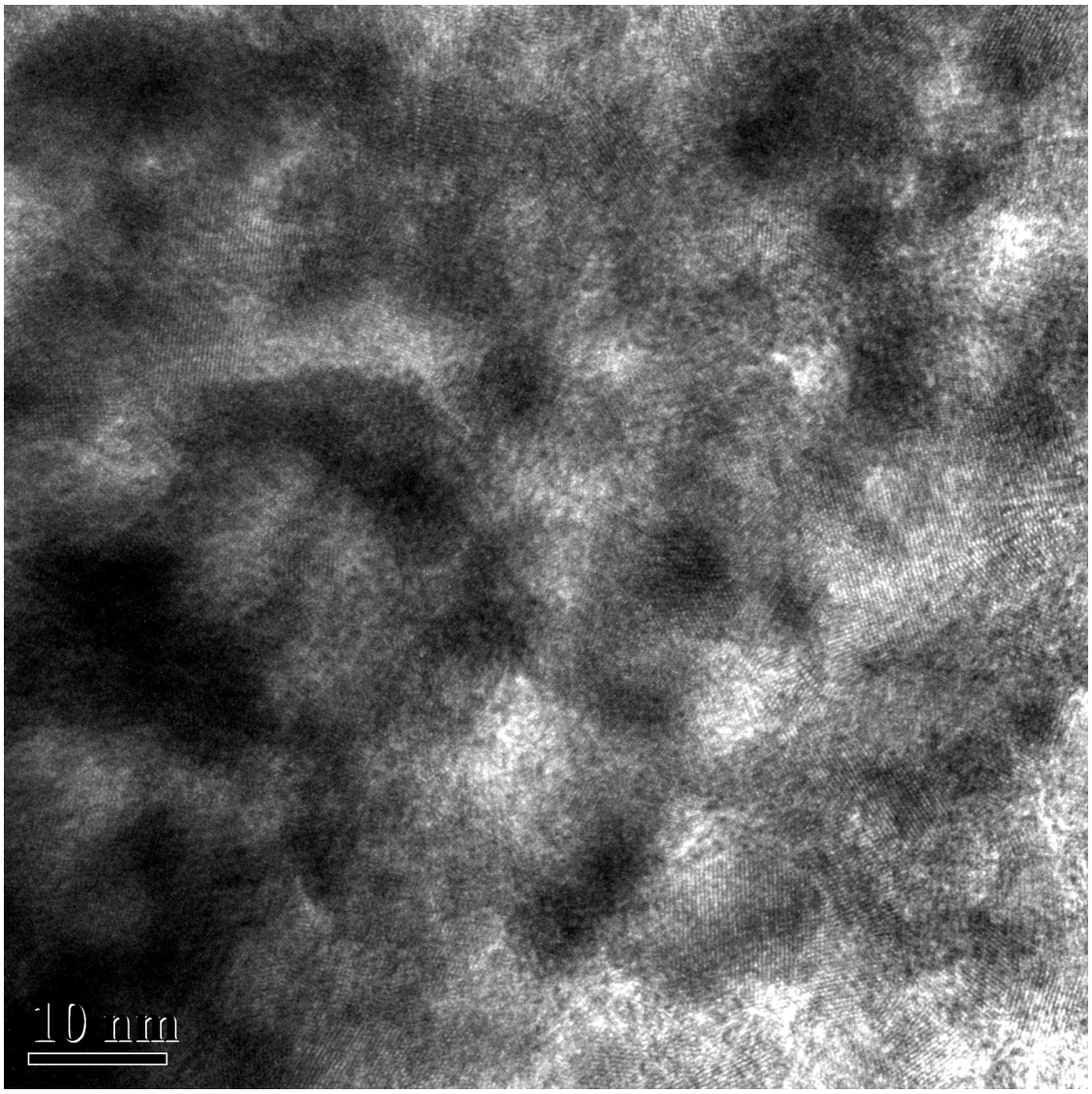

Supplementary Figure S9. TEM image of MCSSNs ultrasonically detached from nanocomposite electrode after 100 charge−discharge cycles.

References

[1] C. M. Hessel, E. J. Henderson and J. G. C. Veinot, *Chem*. *Mater*., **2006**, *18*, 6139.

[2] J. A. Luna-López, G. García-Salgado, T. Díaz-Becerril, J. Carrillo López, D. E. Vázquez-Valerdi, H. Juárez-Santiesteban, E. Rosendo-Andrés and A. Coyopol, *Mater*. *Sci*. *Eng*. *B*, **2010**, *174*, 88.